GLOBAL TESTING AGAINST SPARSE ALTERNATIVES IN TIME-FREQUENCY ANALYSIS[1]

BY T. TONY CAI, YONINA C. ELDAR AND XIAODONG LI

*University of Pennsylvania, Technion—Israel Institute of Technology
and University of California, Davis*

In this paper, an *over-sampled periodogram higher criticism* (OPHC) test is proposed for the global detection of sparse periodic effects in a complex-valued time series. An explicit minimax detection boundary is established between the rareness and weakness of the complex sinusoids hidden in the series. The OPHC test is shown to be asymptotically powerful in the detectable region. Numerical simulations illustrate and verify the effectiveness of the proposed test. Furthermore, the periodogram over-sampled by $O(\log N)$ is proven universally optimal in global testing for periodicities under a mild minimum separation condition.

1. Introduction. In this paper, we study the problem of global testing for periodicity. Suppose $u_t, t = 1, \ldots, N$, is a real-valued time series observed at equispaced time points, that satisfies the model

$$(1.1) \qquad u_t = \sum_{j=1}^{s} a_j \sin(\omega_j t + \phi_j) + \varepsilon_t,$$

where the noise $\varepsilon_t \sim \mathcal{N}(0, \sigma^2)$ are i.i.d. normal variables. In the complex-valued case, similarly, the observed series satisfies the model

$$(1.2) \qquad y_t = \sum_{j=1}^{s} a_j e^{i(\omega_j t + \phi_j)} + z_t,$$

where z_t represents zero-mean i.i.d. complex white noise, that is, $z_t = z_{1t} + i z_{2t}$ with $[z_{1t}, z_{2t}] \sim \mathcal{N}(\mathbf{0}, \frac{\sigma^2}{2}\mathbf{I}_2)$. In both cases, we are interested in testing

$$(1.3) \quad H_0 : a_1 = \cdots = a_s = 0 \quad \text{versus} \quad H_1 : a_j > 0 \qquad \text{for at least one } j,$$

in which periodicity exists in the series under the alternative.

Global detection of periodic patterns in time series analysis have various applications. We give several examples as follows:

Signal detection. Global detection of sinusoidal signals is a fundamental signal processing task prior to information extraction [37, 54, 55]. As summarized in [37], global testing for waveforms can be utilized in radar and sonar systems, such as detecting whether aircrafts are approaching [50] and detecting whether enemy submarines are present [38].

Gene expression studies. Global detection of periodic patterns in time series due to various biological rhythms such as cell division, circadian rhythms, life cycles of microorganisms and many others is an important problem in gene expression studies [1, 2, 17, 30, 56]. For example, in order to identify a collection of genes which are responsible in the cell cycle, it was proposed in [56] to implement global testing of periodicity for each gene expression time series. P-values for these test statistics are subsequently calculated, and then multiple testing is performed based on these p-values while controlling the false discovery rate (FDR) at a prespecified level, so that periodically expressed genes are identified. Further improvements of this method appear in [1, 2, 17, 30] and references therein.

Global testing for periodicity dates back to the well-known Fisher's test [27], which is based on the maximum value of the normalized standard periodogram of the observed series. This test enjoys some optimality properties as long as there is only one sinusoid under the alternative and its frequency lies on the Fourier grid $(0, \frac{2\pi}{N}, \frac{4\pi}{N}, \ldots, \frac{2(N-1)\pi}{N})$. Since then substantial extensions and improvements have been made in the literature. Based on an adaptive set of largest normalized standard periodogram values, an extension of Fisher's test was proposed in [49]. It is empirically shown to be more powerful than Fisher's test when there are multiple periodicities with Fourier frequencies under the alternative. In [19], a modified Fisher's test, in which the maximum periodogram is normalized by a trimmed mean of the periodograms (as suggested in [8]), was proposed and analyzed. This test is also more powerful than Fisher's test when there are multiple periodicities under the alternative. In [20], a test statistic was proposed against the alternative when there is a single sinusoid whose frequency is unknown and not necessarily on the Fourier grid. A more general hypothesis test is given in [36], where the signal of interest consists of a fixed number of sinusoids. The higher criticism test proposed in [23] can also be applied to the standard periodogram for global detection, and it enjoys certain asymptotic minimaxity properties against alternatives in which the periodicities are sparse and consist of Fourier frequencies.

In the existing literature on global testing for periodicity, either the contributing sinusoids are constrained to have Fourier frequencies, or the number of periodicities is fixed and small compared to the sample size. The goal of the present paper is to construct a new test based on an *over-sampled periodogram* that adapts to *a growing number of* sinusoids with *general* frequencies. The focus of our work is to establish the asymptotic optimality of our method.

1.1. *Methodology.* Our discussion throughout the paper is focused on complex-valued time series. As indicated in Section 4.1 of [9] and Section 1.5 of [28], complex-valued time series are sometimes more convenient for analysis. Moreover, complex-valued or bivariate time series arise naturally in modern data analysis such as functional MRI, blood-flow and oceanography; see, for example, [47, 51] and the references therein. Periodicity detection in real-valued series will be briefly discussed in Section 4.

For ease of analysis, we slightly simplify the complex time series model (1.2) as follows:

$$(1.4) \qquad \mathbf{y} = \mathbf{X}\boldsymbol{\beta} + \mathbf{z},$$

where the design matrix $\mathbf{X} \in \mathbb{C}^{N \times p}$ with $p \gg N$ is an *extended discrete Fourier transform* (EDFT) matrix, that is,

$$(1.5) \qquad X_{jk} := \frac{1}{\sqrt{p}} e^{-2\pi i (k-1)(j-1)/p}, \qquad j = 1, \dots, N, k = 1, \dots, p.$$

The vector of coefficients $\boldsymbol{\beta} \in \mathbb{C}^p$ contains information of magnitudes and phases in (1.2), and its sparsity under the alternative, denoted as s, is assumed to be *unknown*. The noise level σ is assumed to be known, and we let $\sigma = 1$ throughout the paper without loss of generality.

A distinct feature of our model in (1.4) is that the value of p can be arbitrarily large, and is assumed to be *unknown*. This implies that the design matrix $\mathbf{X}$ is actually unavailable. Moreover, adjacent columns in $\mathbf{X}$ are nearly parallel, which is different from the common assumption in high-dimensional regression models in which the columns of the design matrices are pairwise incoherent. A broad class of combinations of periodicities can be represented by the mean $\mathbf{X}\boldsymbol{\beta}$. When $\boldsymbol{\beta}$ is s-sparse, $\mathbf{X}\boldsymbol{\beta}$ is a superposition of s complex sinusoids. The global test for periodicity is therefore modeled as

$$(1.6) \qquad H_0 : \boldsymbol{\beta} = \mathbf{0} \quad \text{versus} \quad H_1 : \boldsymbol{\beta} \neq \mathbf{0} \quad \text{and} \quad \boldsymbol{\beta} \text{ is sparse}.$$

We now define the over-sampled periodogram for complex-valued time series, which turns out to be surprisingly simple. For some integer q, define

$$(1.7) \qquad \mathbf{U} = \left(\frac{1}{\sqrt{N}} e^{2\pi i (m-1)(j-1)/q} \right)_{1 \leq m \leq q, 1 \leq j \leq N}$$

whose row vectors are normalized in 2-norm, and set

$$(1.8) \qquad \mathbf{v} = \mathbf{U}\mathbf{y} \quad \text{and} \quad I_m = |v_m|^2, \qquad m = 1, \dots, q.$$

By letting $q > N$, $\{I_1, \dots, I_q\}$ is an over-sampled periodogram. Define

$$(1.9) \qquad \text{HC}(t) := \frac{\sum_{m=1}^q 1_{\{\sqrt{I_m} \geq t\}} - q \bar{\Psi}(t)}{\sqrt{q \bar{\Psi}(t)(1 - \bar{\Psi}(t))}},$$

where $\bar{\Psi}(t) = \mathbb{P}(|z| \geq t) = e^{-t^2}$ is the tail probability of the standard complex normal variable as shown in Lemma 5.2, and I_m is defined in (1.8). Notice that under the null, all v_m are standard complex-valued normal variables, which implies $\mathbb{E}HC(t) = 0$ for any fixed t. The proposed test statistic is defined as

$$(1.10) \qquad \qquad HC^* = \sup_{a \leq t \leq b} HC(t),$$

for which appropriate choices of the interval $[a, b]$ are discussed in Sections 2 and 3. We will fix a threshold level T, and reject H_0 if and only if $HC^* > T$. This test is referred to as the *over-sampled periodogram higher criticism* (OPHC) test.

An important question is how to choose the over-sampling rate q/N. Let $\boldsymbol{\theta} = \mathbb{E}\mathbf{v} = \mathbf{U}\mathbf{X}\boldsymbol{\beta}$. Roughly speaking, the success of detection by the higher criticism based on the sequence $\mathbf{v}$ depends on whether $\boldsymbol{\theta}$ has s nonzero elements with sufficiently large magnitudes. If the frequencies are on the Fourier grid, the spikiness of $\boldsymbol{\theta}$ is implied by the spikiness of $\boldsymbol{\beta}$. For example, if $s = 1$ and

$$y_t = \frac{A}{\sqrt{N}} e^{-i(2\pi/N)t} + z_t,$$

by choosing $q = N$, we can calculate that $\boldsymbol{\theta}$ has sparsity one, and $\|\boldsymbol{\theta}\|_\infty = A$. Therefore, the proposed test is desirable as long as A is sufficiently large. However, if the frequencies are off the Fourier grid, then for $q = N$, the spikiness of $\boldsymbol{\beta}$ may not imply the spikiness of $\boldsymbol{\theta}$. For example, if

$$y_t = \frac{A}{\sqrt{N}} e^{-i(\pi/N)t} + z_t,$$

and one chooses $q = N$, simple calculation yields

$$\limsup_{N \to \infty} \max_{1 \leq m \leq N} |\theta_m| \leq \frac{2}{\pi} A.$$

This means the resulting $\boldsymbol{\theta}$ is not as spiky as in the case where the frequencies are on the Fourier grid, and then the performance of higher criticism based on $\mathbf{v}$ may be not optimal.

In order to increase the spikiness of $\boldsymbol{\theta}$, we propose to choose the over-sampling rate $q/N = O(\log N)$. Our main result Theorem 2.1 guarantees that as long as the frequencies of the complex sinusoids in the mean of $\mathbf{y}$ obey some minimum separation condition, this over-sampling rate leads to an asymptotically optimal global test. A key step in the proof is to show that $\boldsymbol{\theta}$ has s significant nonzero components.[2] In other words, the spikiness of $\boldsymbol{\beta}$ is translated to the spikiness of $\boldsymbol{\theta}$. We emphasize that this over-sampling rate is independent of the grid parameter p and the sparsity s.

---

[2]This is indicated in equation (5.6).

The higher criticism method was originally coined by John Tukey and introduced in Donoho and Jin [23] for signal detection under a sparse homoscedastic Gaussian mixture model, which was previously studied in Ingster [34]. Cai, Jin and Low [13] investigated minimax estimation of the nonnull proportion ε_n under the same model. Hall and Jin [31] proposed a modified version of the high criticism for detection with correlated noise with known covariance matrices. Cai, Jeng and Jin [12] considered heteroscedastic Gaussian mixture model and showed that the optimal detection boundary can be achieved by a double-sided version of the higher criticism test. The papers [4, 6] considered a related problem of detecting a signal with a known geometric shape in Gaussian noise. Cai and Wu [14] studied the detection of sparse mixtures in the setting where the null distribution is known, but not necessarily Gaussian and established the adaptive optimality of the higher criticism for the detection of such general sparse mixtures.

In the special case in which $p = N$, that is, the frequencies are on the grid, the design matrix becomes the orthogonal DFT matrix. Multiplying the measurement by the inverse DFT matrix, the design matrix is reduced to the identity design. Therefore, the problem becomes equivalent to the standard sparse detection model discussed in [23, 34], and the standard higher criticism test proposed in [23] can be directly applied. Notice that in the OPHC test defined above, choosing $q = N$ in (1.7) is equivalent to multiplying the measurement by the inverse DFT, so there is no need to over-sample the periodogram.

1.2. *Relation with global testing in linear models.* If the dimension p in (1.4) were known, the hypothesis testing model (1.4) considered in the present paper is also closely related to the global testing problem under a linear model with sparse alternatives. It is helpful to review some well-known results for the real-valued case in this line of research.

Consider the linear model: $\mathbf{y} = \mathbf{X}\boldsymbol{\beta} + \boldsymbol{\varepsilon}$, where $\mathbf{X} \in \mathbb{R}^{N \times p}$, $\boldsymbol{\beta} \in \mathbb{R}^p$ are the design matrix and regression coefficients, respectively. The noise vector $\boldsymbol{\varepsilon} \in \mathbb{R}^N$ is assumed to be i.i.d. Gaussian variables with mean 0 and variance 1. The global detection of $\boldsymbol{\beta}$ is still captured by the hypothesis test (1.6). In the recently developed literature of high-dimensional statistics, p is comparable or much greater than N, while the parameter vector $\boldsymbol{\beta}$ is assumed to be sparse: $\|\boldsymbol{\beta}\|_0 = s \ll N$. The trade-off between the strength of the nonzero regression coefficients and the sparsity, by which the detectability of $\boldsymbol{\beta}$ is captured, has been intensively studied in the literature.

In order to simplify the analysis, it is convenient to assume that the nonzero components of $\boldsymbol{\beta}$ have the same magnitude A. The tradeoff between the signal strength and sparsity is reduced to a quantitative relationship between A and s for fixed N and p. This relationship also depends closely on the properties of the design matrix $\mathbf{X}$. There are two well-studied examples in the literature:

- Identity design matrix. When $N = p$ and $\mathbf{X} = \mathbf{I}$, the detection boundary is given in [23, 34]. Let $A = \sqrt{2r \log p}$ and $s = p^{1-\alpha}$ with $\alpha \in [\frac{1}{2}, 1]$, a higher criticism test is asymptotically powerful as long as $r > \rho^*(\alpha)$, where the detection boundary function ρ^* is defined as:

$$(1.11) \qquad \rho^*(\alpha) = \begin{cases} (1 - \sqrt{1-\alpha})^2, & \alpha \in [\frac{3}{4}, 1), \\ \alpha - \frac{1}{2}, & \alpha \in (\frac{1}{2}, \frac{3}{4}). \end{cases}$$

On the other hand, if $r < \rho^*(\alpha)$, all sequences of testing procedures are asymptotically powerless, and thus the signal is not detectable. The condition $\alpha > \frac{1}{2}$ is crucial. Otherwise, the detectability of nonzero $\boldsymbol{\beta}$ is not characterized by the scaling $A = \sqrt{2r \log p}$.

- Gaussian design matrix. Another carefully studied class of design matrices are the Gaussian designs; that is, $\mathbf{X} \in \mathbb{R}^{N \times p}$ has i.i.d. zero-mean normal variables with variance $\frac{1}{p}$. This model appears in [35] and [5]. By denoting $A = \sqrt{\frac{2rp \log p}{N}}$ and $s = p^{1-\alpha}$, the detection boundary established in [35] is still $r = \rho^*(\alpha)$ as in the case of identity design, provided $p^{1-\alpha} \log(p) = o(\sqrt{N})$. A similar result is established in [5].

For ease of presentation, we assume $N = p^{1-\gamma}$ with $0 \le \gamma < 1$ throughout the paper. Then in the case of Gaussian designs, the detection boundary $r = \rho^*(\alpha)$ holds when $(1 + \gamma)/2 < \alpha < 1$. However, there is an "unnatural" property of the detection boundary ρ^* in this case: When $\gamma > 0$, $r \to \rho^*(\frac{1+\gamma}{2}) > 0$ as $\alpha \to \frac{1+\gamma}{2}$. In Section 2, with a similar setup of γ, α and r, under the condition $\frac{1+\gamma}{2} < \alpha < 1$, a new detection boundary is developed for the model (1.4) with EDFT designs, as long as the support of $\boldsymbol{\beta}$ satisfies a mild minimum separation condition. To be specific, the new detection boundary is defined as

$$(1.12) \qquad \rho_\gamma^*(\alpha) = \begin{cases} (\sqrt{1-\gamma} - \sqrt{1-\alpha})^2, & \alpha \in \left[\frac{3}{4} + \frac{\gamma}{4}, 1\right), \\ \alpha - \frac{1}{2} - \frac{\gamma}{2}, & \alpha \in \left[\frac{1+\gamma}{2}, \frac{3}{4} + \frac{\gamma}{4}\right). \end{cases}$$

It enjoys the property $r \to \rho_\gamma^*(\frac{1+\gamma}{2}) = 0$ as $\alpha \to \frac{1+\gamma}{2}$. A detailed comparison between the detection boundary of EDFT designs and that of Gaussian designs is also provided in Section 2.

1.3. *Structure of the paper.* The rest of the paper is organized as follows: In Section 2, we give theoretical results for the proposed method. An explicit detection boundary $r = \rho_\gamma^*(\alpha)$ is established under a mild minimum separation assumption on the underlying frequencies, and the asymptotic optimality of OPHC is established. In Section 3, numerical simulations illustrate the efficacy of our approach. In the implementation of OPHC, we compare the performances between

$q/N = O(\log N)$, $q = N$ and $q = p$. A summary of our main contributions is given in Section 4, along with some future research directions. All the proofs are deferred to Section 5.

2. Theoretical results. In this section, we aim to establish a sharp tradeoff between the magnitudes and number of the nonzero components in $\boldsymbol{\beta}$, such that the OPHC test can successfully reject the null hypothesis when the alternative is true. Under the alternative, we assume $\mathrm{supp}(\boldsymbol{\beta}) = \{\tau_1, \ldots, \tau_s\}$, where $1 \leq \tau_1 < \cdots < \tau_s \leq p$. This implies that the nonzero components of $\boldsymbol{\beta}$ are $\beta_{\tau_1}, \ldots, \beta_{\tau_s}$. If we denote $\boldsymbol{\tau} = [\tau_1, \ldots, \tau_s]^T$ and

$$(2.1) \qquad \tilde{\boldsymbol{\beta}} = [\tilde{\beta}_1, \ldots, \tilde{\beta}_s]^T := [\beta_{\tau_1}, \ldots, \beta_{\tau_s}]^T,$$

then under the alternative, the s-sparse signal $\boldsymbol{\beta}$ is uniquely parameterized by $(\boldsymbol{\tau}, \tilde{\boldsymbol{\beta}})$. The distribution of the measurement $\mathbf{y}$ under the alternative is therefore parameterized by $\boldsymbol{\tau}$ and $\tilde{\boldsymbol{\beta}}$, denoted as $\mathbb{P}_{(\boldsymbol{\tau}, \tilde{\boldsymbol{\beta}})}$. Under the null, $\mathbf{y}$ consists of standard complex normal variables, denoted as $\mathbb{P}_0$.

As discussed in Section 1.2, throughout the paper, let $N = p^{1-\gamma}$ with fixed $\gamma \in [0, 1)$, and $s = p^{1-\alpha}$ with $\frac{1+\gamma}{2} < \alpha < 1$. This implies that $s < N^{1/2}$, which is consistent with the assumption in [5, 35].

2.1. *Minimum separation condition.* We assume the distances between the indices of the nonzero components of $\boldsymbol{\beta}$, that is, $\tau_1, \ldots, \tau_s$, satisfy the following minimum separation condition:

$$(2.2) \quad \Delta(\boldsymbol{\tau}) := \frac{1}{p} \min\{|\tau_{l+1} - \tau_l| : l = 1, \ldots, s, \tau_{s+1} := \tau_1 + p\} \geq \frac{\log^2 N}{N}.$$

A similar minimum separation condition appears in the literature of super-resolution; see [16, 24].

This spacing condition holds asymptotically if the support is assumed to be random. Assume that $\tau_1 \leq \cdots \leq \tau_s$ are the order statistics of independent uniformly distributed random variables $a_1, \ldots, a_s$ in $\{1, \ldots, p\}$. For any $a, b \in \{1, \ldots, p\}$, define the distance

$$(2.3) \qquad d(a, b) = \min(|a - b|/p, 1 - |a - b|/p).$$

It is evident that $\Delta(\boldsymbol{\tau}) = \min_{1 \leq l_1 < l_2 \leq s} d(a_{l_1}, a_{l_2})$. For any fixed $l_1 < l_2$, and any $p_0 \in [0, 1]$, it is easy to see $\mathbb{P}(d(a_{l_1}, a_{l_2}) < p_0) \leq 2p_0 + \frac{1}{p}$. Since there are $\frac{s(s-1)}{2}$ pairs, we have

$$\mathbb{P}\left(\min_{1 \leq l_1 < l_2 \leq s} d(a_{l_1}, a_{l_2}) < p_0\right)$$

$$\leq \sum_{1 \leq l_1 < l_2 \leq s} \mathbb{P}(d(a_{l_1}, a_{l_2}) < p_0) \leq s(s-1)\left(p_0 + \frac{1}{2p}\right).$$

By letting $p_0 = \frac{\log^2 N}{N}$, we obtain $\mathbb{P}(\Delta(\boldsymbol{\tau}) < \frac{\log^2 N}{N}) \leq \frac{s^2 \log^2 N}{N} + \frac{s^2}{p}$. Recall that we assume the sparsity satisfies $\frac{1+\gamma}{2} < \alpha < 1$, where $N = p^{1-\gamma}$ and $s = p^{1-\alpha}$. Then $\frac{s^2 \log^2 N}{N} + \frac{s^2}{p} \to 0$ as $p \to \infty$. Therefore, (2.2) holds with probability tending to 1. A simple corollary is that with probability approaching 1, all the indices $a_1, \ldots, a_s$ are distinct.

2.2. *Detection boundary.* Recall that under the alternative, the distribution of the observation $\mathbf{y}$ is parameterized by $(\boldsymbol{\tau}, \tilde{\boldsymbol{\beta}})$. We assume that[3]

(2.4)
$$(\boldsymbol{\tau}, \tilde{\boldsymbol{\beta}}) \in \Gamma(p, N, s, r)$$
$$:= \left\{ |\tilde{\beta}_1| = \cdots = |\tilde{\beta}_s| = A = \sqrt{\frac{rp \log p}{N}}, \Delta(\boldsymbol{\tau}) \geq \frac{\log^2 N}{N} \right\}.$$

For the parameter space $\Gamma(p, N, s, r)$, we aim to establish a new minimax detection boundary $r = \rho_\gamma^*(\alpha)$ defined as in (1.12), when the sparsity level satisfies $\frac{1+\gamma}{2} < \alpha < 1$. Recall that the OPHC test defined by (1.7)–(1.10) is determined by the interval $[a, b]$, the specific choice of $q = O(N \log N)$, and the threshold T. In our theoretical analysis, we choose $q = N \lfloor \log N + 1 \rfloor$, $[a, b] = [1, \sqrt{\log \frac{N}{3}}]$, and $T = \log^2 N$. The OPHC test is therefore defined as

(2.5)
$$\Psi = I\left(\mathrm{HC}^* > \log^2 N\right).$$

That is, the null hypothesis is rejected if and only if $\mathrm{HC}^* > \log^2 N$. This threshold is often too conservative in practice, and a more reliable and useful threshold for finite samples can be chosen by Monte Carlo simulations, which we will discuss in Section 3.

Our first theorem is regarding the detectable region of (α, r), in which the null can be successfully rejected asymptotically.

THEOREM 2.1. *In the measurement model* (1.4), *suppose* $N = p^{1-\gamma}$ *with* $\gamma \in [0, 1)$. *Under the alternative, we assume* $s = p^{1-\alpha}$ *with* $\frac{1+\gamma}{2} < \alpha < 1$, *and* $(\boldsymbol{\tau}, \tilde{\boldsymbol{\beta}})$ *satisfies* (2.4) *with parameter* r. *Suppose* ρ_γ^* *is defined as in* (1.12). *If* $r > \rho_\gamma^*(\alpha)$, *the OPHC test defined by* (1.7)–(1.10) *with* $q = N \lfloor \log N + 1 \rfloor$ *and* $[a, b] = [1, \sqrt{\log \frac{N}{3}}]$ *is asymptotically powerful:*

$$\lim_{N \to \infty} \left(\mathbb{P}_0(H_0 \text{ is rejected}) + \max_{(\boldsymbol{\tau}, \tilde{\boldsymbol{\beta}}) \in \Gamma(p, N, s, r)} \mathbb{P}_{(\boldsymbol{\tau}, \tilde{\boldsymbol{\beta}})}(H_0 \text{ is accepted}) \right) = 0.$$

---

[3]As discussed in Section 1.2, it is assumed that $A = \sqrt{\frac{2rp \log p}{N}}$ in the literature of global detection boundaries under linear models. The difference of $\sqrt{2}$ stems from the difference between real-valued and complex-valued sequences.

The most significant technical novelty in this paper lies in the proof of Theorem 2.1. In the analysis of HC* under the alternative, the mean and covariance structure of $\mathbf{v}$, which is defined in (1.8), requires more careful calculation than in existing work, for example, [5, 31]. In particular, the estimation of $\mathbb{E}(v_1), \ldots, \mathbb{E}(v_q)$ and the control of $\mathrm{Cov}(1_{|v_a|>t}, 1_{|v_b|>t})$ are treated cautiously based on a variety of cases. In relevant calculations, the structure of the EDFT design matrix $\mathbf{X}$ needs to be sufficiently employed. Under the null, the HC* statistic is related to the standard HC* statistic discussed in [23], so the analysis is easier than the case of alternative.

The following theorem gives the lower bound for the testing problem.

THEOREM 2.2. *Under the same setup of Theorem* 2.1, *if* $r < \rho_\gamma^*(\alpha)$, *then all sequences of hypothesis tests are asymptotically powerless, that is,*

$$\lim_{N \to \infty} \left(\mathbb{P}_0(H_0 \text{ is rejected}) + \max_{(\boldsymbol{\tau}, \tilde{\boldsymbol{\beta}}) \in \Gamma(p, N, s, r)} \mathbb{P}_{(\boldsymbol{\tau}, \tilde{\boldsymbol{\beta}})}(H_0 \text{ is accepted}) \right) = 1.$$

The proof of Theorem 2.2 is relatively easy, and it is given in the supplemental material. In fact, by taking advantage of the specific structure of the EDFT matrix $\mathbf{X}$, the deduction can be reduced to the case $\mathbf{X} = \mathbf{I}$. The classic lower bound arguments in [23, 31, 34] can then be directly applied.

Theorems 2.1 and 2.2 together show that the proposed test is asymptotically optimal. We now compare ρ_γ^* with the detection boundary ρ^* associated with the Gaussian designs established in [5]. As indicated in Section 1.3, after normalizing the rows of the Gaussian design, the magnitude parameter is denoted as $A = \sqrt{\frac{2rp \log p}{N}}$. Notice that in our model the magnitude parameter is $A = \sqrt{\frac{rp \log p}{N}}$, and the difference of $\sqrt{2}$ is due to the distinction between real-valued and complex-valued models. Therefore, it is fair to compare ρ^* and ρ_γ^* directly. It is obvious that $\rho_\gamma^*(\alpha) < \rho^*(\alpha)$ for all $\frac{1+\gamma}{2} < \alpha < 1$ as long as $\gamma > 0$. This implies that the detection boundary associated with the extended DFT design matrix leads to milder trade-off between the rareness and the weakness of the nonzero components of $\boldsymbol{\beta}$ than that of Gaussian designs. To illustrate their differences, the two detection boundary functions are plotted in Figure 1 for $\gamma = 0.3$.

3. Numerical simulations. In this section, we study the empirical behavior of the OPHC test by numerical simulations. In terms of computation, it is more convenient to express the statistic as a function of $P_{(1)} \le P_{(2)} \le \cdots \le P_{(q)}$, which are the ordered P-values of $|v_1|, \ldots, |v_q|$, that is, $P_m := \bar{\Psi}(|v_m|) = e^{-|v_m|^2}$. The HC* test in the following numerical simulations is defined as

$$(3.1) \qquad \mathrm{HC}^* = \max_{m: 1/q \le P_{(m)} < 1/2} \frac{m - q P_{(m)}}{\sqrt{q P_{(m)}(1 - P_{(m)})}},$$
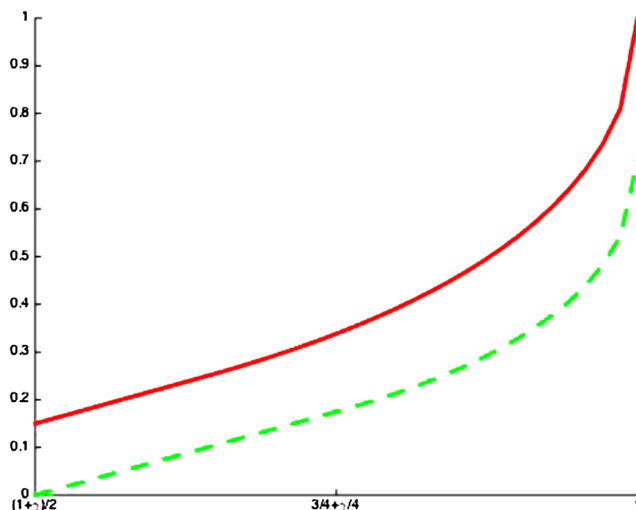
FIG. 1.   *Detection boundary functions $\rho^*(\alpha)$ (red solid line) and $\rho_\gamma^*(\alpha)$ (green dashed line) for $\gamma = 0.3$ and $\frac{1+\gamma}{2} < \alpha < 1$.*

which is equivalent to choosing $[a, b] = [\sqrt{\log 2}, \sqrt{\log q}]$ in (1.10), instead of the theoretical choice $[a, b] = [1, \sqrt{\log \frac{N}{3}}]$ defined in Section 2.

In the following, we compare the empirical testing powers of the OPHC test with various choices of q.

First, let $N = 1000$ and $q = 2N \lfloor \log N + 1 \rfloor = 14{,}000$. Then the empirical distribution of the OPHC test statistic HC* under the null can be derived by Monte Carlo simulation with 1000 independent trials, which is shown in the upper panel of Figure 2.

Under the alternative, we assume that $p = 1{,}000{,}000$ and $s = 20$. The support of $\boldsymbol{\beta}$ is distributed uniformly at random, and the phase of the nonzero entries of $\boldsymbol{\beta}$ are uniformly distributed on $[0, 2\pi)$. All nonzero components of $\boldsymbol{\beta}$ have the same magnitude $A = \sqrt{\frac{rp \log p}{N}}$ with $r = 0.3$.

We first assume that the variance $\sigma^2 = 1$ is known. The resulting empirical distribution of HC* under the mixed alternative is plotted in the middle panel of Figure 2 by 1000 independent trials. In 956 trials of them, the empirical P-values are smaller than 0.05, by which the periodicities are successfully detected.

Let us discuss the case where the variance $\sigma^2 = 1$ is unknown. Since it is necessary to make sure that the estimation of the variance is consistent under the null, we use the mean square of $|y_t|$ as the estimate. This estimator of σ is adopted in order to make fair numerical comparisons between different choices of q. Robust and efficient estimation of σ is an interesting problem. It has been considered, for example, in [21], in the case of Gaussian design. Efficient estimation of σ in the current setting is beyond the scope of this paper, and we leave it for future re-
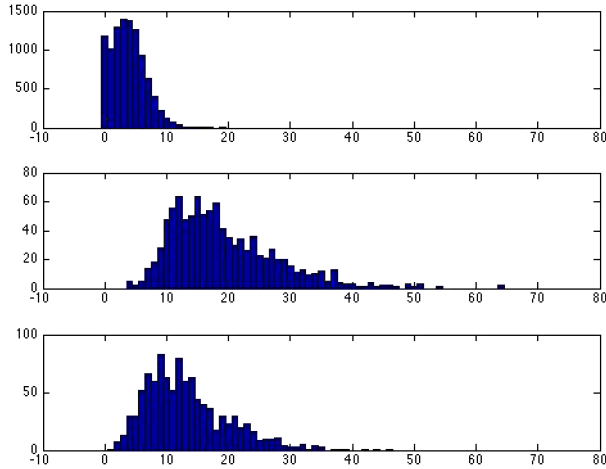
FIG. 2.   *Empirical distribution of the OPHC test statistic under the null is plotted in the upper panel, where $N = 1000$ and $q = 14{,}000$. Under the mixed alternative, we let $p = 1{,}000{,}000$, $s = 20$ and $r = 0.3$. Empirical distribution of the OPHC test statistic is plotted in the middle panel with known $\sigma = 1$, and in the lower panel with estimated variance of noise.*

search. The resulting empirical distribution of HC* is plotted in the lower panel of Figure 2. Among the 1000 trials, there are 745 with empirical P-values smaller than 0.05.

Next, we consider the OPHC test with $q = N = 1000$. We refer to this test as standard periodogram higher criticism (SPHC) test. The empirical distribution of the SPHC test statistic under the null is plotted in the upper panel of Figure 3. The setup of the mixed alternative is the same as in the experiments for the OPHC test described before. Suppose the variance $\sigma^2 = 1$ is known. The distribution of the SPHC test statistic under the alternative is plotted in the middle panel of Figure 3 by 1000 trials. In 867 trials of them, the empirical P-values are smaller than 0.05. This is worse than the OPHC method with $q = 14{,}000$, where the periodicities are successfully detected in 956 trials. When the variance of the noise is unknown, we still estimate it by the mean square of $|y_t|$, such that the estimate is consistent under the null. The resulting empirical distribution of the SPHC test statistic is plotted in the lower panel of Figure 3 based on 1000 independent trials. In only 478 trials among them, the empirical P-values are smaller than 0.05. This is also worse than OPHC where the periodicities are successfully detected in 745 independent trials.

Finally, we assume p were known and consider the OPHC test with $q = p = 1{,}000{,}000$. In this case the OPHC test coincides with the method proposed in [5]. The empirical distribution of this test statistic under the null by 1000 independent trials is plotted in the upper panel of Figure 4. The setup of the mixed alternative is the same as before. When the variance $\sigma^2 = 1$ is known, the distribution of this test statistic under the alternative is plotted in the middle panel of Figure 4 by 1000 trials. In 949 trials of them, the empirical P-values are smaller than 0.05, which
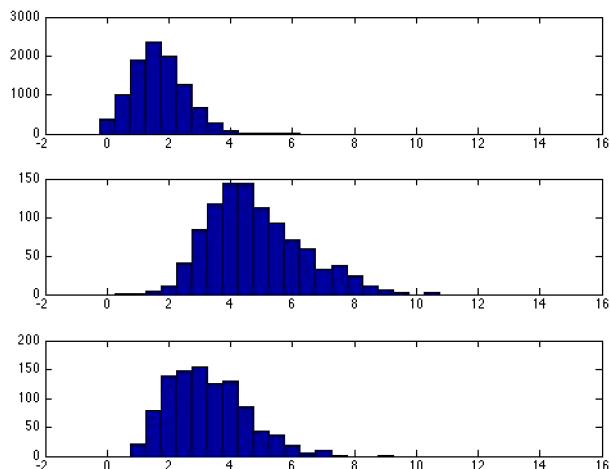
FIG. 3. *Empirical distribution of the SPHC test statistic under the null is plotted in the upper panel, where $N = 1000$ and $q = 1000$. Under the mixed alternative, we let $p = 1,000,000$, $s = 20$ and $r = 0.3$. Empirical distribution of the SPHC test statistic is plotted in the middle panel with known $\sigma = 1$, and in the lower panel with estimated variance of noise.*

is slightly worse than the OPHC method with $q = 14,000$ as mentioned before. When the variance of the noise is unknown, with its estimation by the mean square of $|y_t|$, the resulting empirical distribution of this test statistic is plotted in the lower panel of Figure 4 based on 1000 independent trials. In 741 trials among them, the
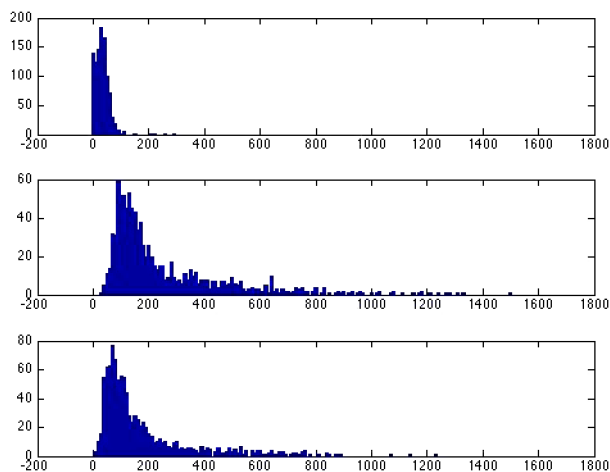

FIG. 4. *Empirical distribution of the OPHC test statistic under the null is plotted in the upper panel, where $N = 1000$ and $q = 1,000,000$. Under the mixed alternative, we let $p = 1,000,000$, $s = 20$ and $r = 0.3$. Empirical distribution of this test statistic is plotted in the middle panel with known $\sigma = 1$, and in the lower panel with estimated variance of noise.*

empirical P-values are smaller than 0.05, which is also slightly worse than the OPHC method with $q = 14,000$. Since p is actually unknown, it would be more convenient to choose $q = O(N \log N)$.

4. Discussion. Motivated by periodicity detection in complex-valued time series analysis, we investigated the hypothesis testing problem (1.6) under the linear model (1.4), where the frequencies of the hidden periodicities are not necessarily on the Fourier grid, and the number of sinusoids grows in N. The OPHC test, a higher criticism test applied to the periodogram over-sampled by $O(\log N)$, is proposed to solve this problem. In terms of theory, by assuming that the frequencies satisfy a minimum separation condition, a detection boundary between the rareness and weakness of the sinusoids is explicitly established. Perhaps surprisingly, the detectable region for the EDFT design matrix is broader than that of Gaussian design matrices. For ease of exposition, we assume that p is finite but unknown, although p is allowed to be infinity by slightly modifying our argument.

Numerical simulations validate the choice $q = O(N \log N)$ by being compared to the choice $q = N$, that is, the standard periodogram higher criticism, and $q = p$, that is, excessively over-sampled periodogram methods. In a recently published paper [40], it is shown that higher criticism statistics might not be as powerful as Berk–Jones statistics empirically. We find it interesting to investigate alternative global testing methods for periodicity detection both theoretically and empirically, but we leave this as future work.

The hypothesis testing problem considered in this paper is related to a number of other interesting problems. We briefly discuss them here, along with several directions for future research.

Statistical estimation of a large number of frequencies. A related important statistical problem is to estimate the frequencies of the periodicities in a given series. Sinusoidal regression methods date back to 1795 by Prony [43] with many later developments including [10, 33, 46, 48], to name a few. In the case where the number of frequencies is fixed and few, numerous statistical analyses for frequency estimation have been performed in the literature. For example, an insightful threshold behavior of MLE was presented in [45]. To determine the number of frequencies, model selection methods are usually applied; see, for example, [22, 42]. An extensive study on this subject can be found in the classical text book [44] and references therein. In contrast, when the number of frequencies is large, although sparse recovery [18, 25, 26, 32] and total-variation minimization [15, 16] can be used for frequency retrieval, their statistical efficiency is not clear. It is interesting to develop both computationally and statistically efficient methods to estimate a number of frequencies hidden in the observed sequence.

Sinusoidal denoising. Compared to frequency estimation, denoising, that is, estimation of the mean $\mathbf{X}\boldsymbol{\beta}$ in (1.4), is a conceptually easier statistical task. In the recent papers [7, 52], SDP methods were shown to enjoy nearly-optimal statistical properties. It would be interesting to establish theoretically optimal methods.

4.1. *Testing for periodicity in real-valued series.* Considering the hypothesis test problem (1.3) in the real case (1.1), the OPHC test can be applied to the real sequence u_t by the idea of complexification, that is, transforming u_t into $y_t = u_t + iu_{t+n}$ for $t = 1, \ldots, n$. Consequently, the mean of y_t amounts to a superposition of complex sinusoids, and the noise part in y_t consists of a sequence of complex white noise. Then the hypothesis test problem is reduced to the complex case. It would be interesting to investigate whether OPHC method can be applied to the real series directly with potential statistical advantage.

5. Proofs. This section is dedicated to the proofs of Theorems 2.1 and 2.2. We begin by collecting a few technical tools that will be used in the proof of the main results.

5.1. *Preliminaries.* First, we formally introduce the concept of complex-valued multivariate normal distribution.

DEFINITION 5.1. We say that $\mathbf{z} = \mathbf{x} + i\mathbf{y} \in \mathbb{C}^n$ is an n-dimensional complex-valued multivariate normal vector with distribution $\mathcal{CN}(\boldsymbol{\mu}, \boldsymbol{\Gamma}, \boldsymbol{\Omega})$, if $\begin{bmatrix} \mathbf{x} \\ \mathbf{y} \end{bmatrix}$ is an $2n$-dimensional real-valued normal vector, and $\mathbf{z}$ satisfies

$$\mathbb{E}\mathbf{z} = \boldsymbol{\mu}, \qquad \mathbb{E}\big((\mathbf{z} - \boldsymbol{\mu})(\mathbf{z} - \boldsymbol{\mu})^*\big) = \boldsymbol{\Gamma}, \qquad \mathbb{E}\big((\mathbf{z} - \boldsymbol{\mu})(\mathbf{z} - \boldsymbol{\mu})^T\big) = \boldsymbol{\Omega}.$$

Here, $\mathbf{X}^*$ denotes the complex conjugate transpose, while $\mathbf{X}^T$ denotes the ordinary transpose. Moreover, we say a complex-valued multivariate normal vector $\mathbf{z}$ is standard, if

$$\mathbf{z} \sim \mathcal{CN}(\mathbf{0}, \mathbf{I}_n, \mathbf{0}).$$

The following lemma gives the tail distribution of the standard complex normal variable, which turns out to be much neater than that of real normal variables. Its proof is given in [11].

LEMMA 5.2. *Suppose $z \sim \mathcal{CN}(0, 1, 0)$ is the standard circularly-symmetric complex normal variable. Then for any $t \geq 0$, $\bar{\Psi}(t) := \mathbb{P}(|z| \geq t) = e^{-t^2}$. In addition, if $\mu \in \mathbb{C}$ is fixed, we have*

$$(5.1) \qquad \frac{C_0}{1 + (t - |\mu|)_+} e^{-(t-|\mu|)_+^2} \leq \mathbb{P}(|\mu + z| > t) \leq e^{-(t-|\mu|)_+^2}$$

for some positive numerical constant C_0. Here, $x_+ := \max(x, 0)$ for $x \in \mathbb{R}$, and x_+^2 is short for $(x_+)^2$.

Under the alternative hypothesis, we need an upper bound of the variance of $HC(t)$ for fixed t, for which the following lemma will be applied for several times. The argument is standard in the literature of normal comparison inequalities; see, for example, [39, 41].

LEMMA 5.3. *Suppose* $\begin{bmatrix} w_1 \\ w_2 \end{bmatrix} \sim \mathcal{CN}(\mathbf{0}, \mathbf{\Gamma}, \mathbf{0})$ *is a 2-dimensional complex normal vector, where* $\mathbf{\Gamma} = \begin{bmatrix} 1 & \xi \\ \bar{\xi} & 1 \end{bmatrix}$.

1. *For any fixed* $a_1, a_2 \in \mathbb{C}$ *and* $t > 0$, *there holds*

$$\mathrm{Cov}(1_{\{|w_1 - a_1| > t\}}, 1_{\{|w_2 - a_2| > t\}}) \leq \min(e^{-(t - |a_1|)^2_+}, e^{-(t - |a_2|)^2_+}).$$

2. *If* $|\xi| \leq \frac{1}{2}$, *we obtain*

$$\mathrm{Cov}(1_{\{|w_1 - a_1| > t\}}, 1_{\{|w_2 - a_2| > t\}})$$

$$\leq C_0 |\xi| \exp\left(-\frac{(t - |a_1|)^2_+ + (t - |a_2|)^2_+}{1 + |\xi|}\right)(1 + (t - |a_1|)_+)(1 + (t - |a_2|)_+)$$

for some positive numerical constant C_0.

The proof of this lemma is given in the supplemental material [11].

LEMMA 5.4. *Suppose* $X_1, \ldots, X_n$ *are* n *i.i.d. random variables uniformly distributed on* $[0, 1]$. *Then*

$$\mathbb{P}\left[\sup_{3/n \leq \rho \leq 1 - 3/n} \frac{|\sum_{j=1}^n 1_{\{X_j \leq \rho\}} - n\rho|}{\log n \sqrt{n\rho(1 - \rho)}} > C_1\right] \leq \frac{1}{\log^2 n}$$

provided $n > N_0$. *Here,* C_1 *and* N_0 *are positive numerical constants.*

PROOF. This is a weak version of existing concentration inequalities in [53] for ratio type empirical processes; see also [3, 29]. □

Finally, there is a simple and useful result which we will use in the proofs for several times.

LEMMA 5.5. *For any* $a, b \in [0, 1]$, *define* $d(a, b) = \min(|a - b|, 1 - |a - b|)$. *We have* $4d(a, b) \leq |1 - e^{2\pi i(a-b)}| \leq 2\pi d(a, b)$.

PROOF. These inequalities can be obtained by comparing the length of arcs and chords in the unit circle. □

5.2. *Proof of Theorem* 2.1. Suppose $\varepsilon > 0$ is an underdetermined positive parameter, which will be specified later in order to establish the detectable region. Denote $L = \lfloor \log N + 1 \rfloor$, and hence $q = NL$. By the definition of $\mathbf{v}$ (1.8) and the definition of $\tilde{\boldsymbol{\beta}}$ (2.1), we have

$$y_j = \frac{1}{\sqrt{p}} \sum_{l=1}^{s} e^{-2\pi i (j-1)(\tau_l - 1)/p} \tilde{\beta}_l + z_j, \qquad j = 1, \ldots, N,$$

and

$$
\begin{aligned}
v_m &= \frac{1}{\sqrt{N}} \sum_{j=1}^{N} e^{2\pi i (m-1)(j-1)/q} y_j \\
&= \frac{1}{\sqrt{Np}} \sum_{j=1}^{N} \sum_{l=1}^{s} e^{2\pi i (j-1)((m-1)/q - (\tau_l - 1)/p)} \tilde{\beta}_l
\end{aligned}
$$

(5.2)

$$
+ \frac{1}{\sqrt{N}} \sum_{j=1}^{N} e^{2\pi i (m-1)(j-1)/q} z_j
$$

$$
:= \theta_m + w_m, \qquad m = 1, \ldots, q.
$$

It is obvious that θ_m is deterministic and $(w_1, \ldots, w_q)$ is a q-dimensional complex multivariate normal vector. First, since $z_j \sim \mathcal{CN}(0, 1, 0)$ are independent, we know $\mathbb{E} z_j^2 = 0$ and $\mathbb{E} z_j \bar{z}_j = 1$. This implies $\mathbb{E} w_m^2 = 0$ and $\mathbb{E} w_m \bar{w}_m = 1$ and, therefore, $w_m \sim \mathcal{CN}(0, 1, 0)$. For any $1 \leq m_1, m_2 \leq q$ and $m_1 \neq m_2$, straightforward calculation gives $\mathbb{E} w_{m_1} w_{m_2} = 0$ and

$$\mathbb{E}(w_{m_1} \bar{w}_{m_2}) = \frac{1}{N} \sum_{j=1}^{N} e^{2\pi i (m_1 - m_2)(j-1)/q} = \frac{1 - e^{2\pi i N (m_1 - m_2)/q}}{N(1 - e^{2\pi i (m_1 - m_2)/q})}.$$

This implies $\begin{bmatrix} w_{m_1} \\ w_{m_2} \end{bmatrix} \sim \mathcal{CN}\left(\mathbf{0}, \begin{bmatrix} 1 & \xi \\ \bar{\xi} & 1 \end{bmatrix}, \mathbf{0}\right)$, where $\xi = \frac{1 - e^{2\pi i N (m_1 - m_2)/q}}{N(1 - e^{2\pi i (m_1 - m_2)/q})}$. For all $m_1 \neq m_2$, by Lemma 5.5,

$$(5.3) \qquad |\xi| \leq \frac{2}{N|1 - e^{2\pi i (m_1 - m_2)/q}|} \leq \frac{1}{2Nd((m_1 - 1)/q, (m_2 - 1)/q)}.$$

Furthermore, when $\frac{m_1 - m_2}{L} = \frac{N(m_1 - m_2)}{q}$ is an integer, we have

$$(5.4) \qquad \xi = \frac{1 - e^{2\pi i N (m_1 - m_2)/q}}{N(1 - e^{2\pi i (m_1 - m_2)/q})} = 0.$$

This implies that w_{m_1} and w_{m_2} are independent.

5.2.1. *Lower bound of* $\mathbb{E}\mathrm{HC}(t)$ *under the alternative.*

Step 1. We choose $m_1, \ldots, m_s \in \{1, \ldots, q\}$ such that $\frac{m_1-1}{q}, \frac{m_2-1}{q}, \ldots, \frac{m_s-1}{q}$ are closest to $\frac{\tau_1-1}{p}, \ldots, \frac{\tau_s-1}{p}$ under the metric d, respectively. This implies that for each $1 \le l \le s$,

$$(5.5) \qquad d\left(\frac{m_l-1}{q}, \frac{\tau_l-1}{p}\right) \le \frac{1}{2q} \le \frac{1}{2N \log N}.$$

Since τ satisfies the minimum separation condition as indicated in (2.4), $m_1, \ldots, m_s$ must be distinct.

Therefore, for $1 \le \nu \le s$,

$$\theta_{m_\nu} = \sum_{\substack{1 \le l \le s \\ l \ne \nu}} \frac{\tilde{\beta}_l}{\sqrt{Np}} \sum_{j=1}^{N} e^{2\pi i (j-1)((m_\nu-1)/q - (\tau_l-1)/p)}$$

$$+ \frac{\tilde{\beta}_\nu}{\sqrt{Np}} \sum_{j=1}^{N} e^{2\pi i (j-1)((m_\nu-1)/q - (\tau_\nu-1)/p)}$$

$$:= S_1 + S_2.$$

First, as to S_1, we have

$$|S_1| = \frac{1}{\sqrt{Np}} \left| \sum_{1 \le l \le s, l \ne \nu} \tilde{\beta}_l \sum_{j=1}^{N} e^{2\pi i (j-1)((m_\nu-1)/q - (\tau_l-1)/p)} \right|$$

$$= \frac{1}{\sqrt{Np}} \left| \sum_{1 \le l \le s, l \ne \nu} \tilde{\beta}_l \frac{1 - e^{2\pi i N((m_\nu-1)/q - (\tau_l-1)/p)}}{1 - e^{2\pi i ((m_\nu-1)/q - (\tau_l-1)/p)}} \right|$$

$$\le \frac{\|\boldsymbol{\beta}\|_\infty}{\sqrt{Np}} \sum_{1 \le l \le s, l \ne \nu} \frac{2}{|1 - e^{i 2\pi ((m_\nu-1)/q - (\tau_l-1)/p)}|}$$

$$\le \frac{\|\boldsymbol{\beta}\|_\infty}{\sqrt{Np}} \sum_{1 \le l \le s, l \ne \nu} \frac{2}{4d((m_\nu-1)/q, (\tau_l-1)/p)}.$$

The last inequality is due to Lemma 5.5. Let us now bound

$$\sum_{1 \le l \le s, l \ne \nu} \frac{2}{4d((m_\nu-1)/q, (\tau_l-1)/p)}.$$

Since

$$d\left(\frac{m_\nu-1}{q}, \frac{\tau_l-1}{p}\right)$$

$$\ge d\left(\frac{\tau_l-1}{p}, \frac{\tau_\nu-1}{p}\right) - d\left(\frac{m_\nu-1}{q}, \frac{\tau_\nu-1}{p}\right)$$

$$\geq \min(|\nu - l|, s - |\nu - l|)\Delta(\boldsymbol{\tau}) - \frac{1}{2q}$$

$$\geq \min(|\nu - l|, s - |\nu - l|)\left(\Delta(\boldsymbol{\tau}) - \frac{1}{2q}\right),$$

we have

$$\sum_{1 \leq l \leq s, l \neq \nu} \frac{2}{4d((m_\nu - 1)/q, (\tau_l - 1)/p)}$$

$$\leq \left(\sum_{a=1}^{\lfloor s/2 \rfloor} \frac{1}{a}\right) \frac{1}{\Delta(\boldsymbol{\tau}) - 1/(2q)} \leq \frac{\log s}{\Delta(\boldsymbol{\tau}) - 1/(2q)}.$$

As a result $|S_1| \leq \frac{\|\boldsymbol{\beta}\|_\infty}{\sqrt{Np}} \frac{\log s}{\Delta(\boldsymbol{\tau}) - 1/(2q)}$. As to S_2, we have

$$\left|S_2 - \frac{\sqrt{N}\tilde{\beta}_\nu}{\sqrt{p}}\right| = \frac{\tilde{\beta}_\nu}{\sqrt{Np}}\left(\sum_{j=1}^{N} e^{2\pi i(j-1)((m_\nu-1)/q - (\tau_\nu-1)/p)} - N\right)$$

$$\leq \frac{\|\boldsymbol{\beta}\|_\infty}{\sqrt{Np}} \sum_{j=1}^{N} |e^{2\pi i(j-1)((m_\nu-1)/q - (\tau_\nu-1)/p)} - 1|$$

$$= \frac{\|\boldsymbol{\beta}\|_\infty}{\sqrt{Np}} \sum_{j=1}^{N} |e^{2\pi i(j-1)d((m_\nu-1)/q, (\tau_\nu-1)/p)} - 1|.$$

The last inequality is by the definition of d in Lemma 5.5. By (5.5), we have $d(\frac{m_\nu-1}{q}, \frac{\tau_\nu-1}{p}) \leq \frac{1}{2q}$. By Lemma 5.5, there holds

$$|e^{2\pi i(j-1)d((m_\nu-1)/q, (\tau_\nu-1)/p)} - 1| \leq d\left((j-1)2\pi d\left(\frac{m_\nu-1}{q}, \frac{\tau_\nu-1}{p}\right), 0\right)$$

$$\leq \frac{(j-1)\pi}{q}.$$

This implies that

$$\left|S_2 - \frac{\sqrt{N}\tilde{\beta}_\nu}{\sqrt{p}}\right| \leq \frac{\|\boldsymbol{\beta}\|_\infty}{\sqrt{Np}} \frac{\pi}{q} \frac{N(N-1)}{2}.$$

In summary,

$$\left|\theta_{m_\nu} - \sqrt{\frac{N}{p}}\tilde{\beta}_\nu\right| \leq \frac{\|\boldsymbol{\beta}\|_\infty}{\sqrt{Np}}\left(\frac{\log s}{\Delta(\boldsymbol{\tau}) - 1/(2q)} + \frac{\pi N(N-1)}{2q}\right)$$

$$\leq \frac{\sqrt{r \log p}}{N}\left(\frac{\log s}{(\log^2 N)/N - 1/(2N \log N)} + \frac{\pi N(N-1)}{2N \log N}\right).$$

Noticing $N = p^{1-\gamma}$ and $s = p^{1-\alpha}$, for any fixed $\varepsilon > 0$, we have

$$(5.6) \qquad \left| \theta_{m_\nu} - \sqrt{\frac{N}{p}} \tilde{\beta}_\nu \right| \leq \varepsilon^2 \sqrt{r \log p}, \qquad \nu = 1, \ldots, s,$$

provided $p > C(\gamma, \alpha, r, \varepsilon)$, which is a constant only depending on γ, α, r and ε.

Step 2. Define $D_l \subset \{1, \ldots, q\}$ for $1 \leq l \leq s$ as

$$D_l = \left\{ m : 1 \leq m \leq q, d\left(\frac{m}{q}, \frac{\tau_l}{p}\right) < \frac{\sqrt{\log N}}{N} \right\},$$

and $D = \bigcup_{1 \leq l \leq s} D_l$. Since $\Delta(\boldsymbol{\tau}) \geq \frac{\log^2 N}{N} > \frac{2\sqrt{\log N}}{N}$, $D_1, \ldots, D_s$ are disjoint subsets of $\{1, \ldots, q\}$. For each index $m \in D_\nu$, $\nu = 1, \ldots, s$, since

$$\theta_m = \sum_{\substack{1 \leq l \leq s \\ l \neq \nu}} \frac{\tilde{\beta}_l}{\sqrt{Np}} \sum_{j=1}^{N} e^{2\pi i (j-1)((m-1)/q - (\tau_l - 1)/p)}$$

$$+ \frac{\tilde{\beta}_\nu}{\sqrt{Np}} \sum_{j=1}^{N} e^{2\pi i (j-1)((m-1)/q - (\tau_\nu - 1)/p)},$$

we have

$$|\theta_m| \leq \left| \frac{\tilde{\beta}_\nu}{\sqrt{Np}} \sum_{j=1}^{N} e^{2\pi i (j-1)((m-1)/q - (\tau_\nu - 1)/p)} \right|$$

$$+ \left| \sum_{\substack{1 \leq l \leq s \\ l \neq \nu}} \frac{\tilde{\beta}_l}{\sqrt{Np}} \sum_{j=1}^{N} e^{2\pi i (j-1)((m-1)/q - (\tau_l - 1)/p)} \right|$$

$$\leq \sqrt{\frac{N}{p}} \|\boldsymbol{\beta}\|_\infty + \frac{\|\boldsymbol{\beta}\|_\infty}{\sqrt{Np}} \sum_{\substack{1 \leq l \leq s \\ l \neq \nu}} \frac{|1 - e^{2\pi i N((m-1)/q - (\tau_l - 1)/p)}|}{|1 - e^{2\pi i ((m-1)/q - (\tau_l - 1)/p)}|}$$

$$\leq \sqrt{\frac{N}{p}} \|\boldsymbol{\beta}\|_\infty + \frac{\|\boldsymbol{\beta}\|_\infty}{\sqrt{Np}} \sum_{\substack{1 \leq l \leq s \\ l \neq \nu}} \frac{1}{2 d((m-1)/q, (\tau_l - 1)/p)}.$$

Notice that

$$d\left(\frac{m-1}{q}, \frac{\tau_l - 1}{p}\right) \geq d\left(\frac{\tau_\nu - 1}{p}, \frac{\tau_l - 1}{p}\right) - d\left(\frac{m-1}{q} - \frac{\tau_\nu - 1}{p}\right)$$

$$\geq \min(|\nu - l|, r - |\nu - l|)\Delta(\boldsymbol{\tau}) - \frac{\sqrt{\log N}}{N}$$

$$\geq \min(|\nu - l|, r - |\nu - l|)\left(\Delta(\boldsymbol{\tau}) - \frac{\sqrt{\log N}}{N}\right).$$

This implies that

$$\sum_{\substack{1 \le l \le s \\ l \neq v}} \frac{1}{2d((m-1)/q, (\tau_l - 1)/p)}$$

$$\le \left(\sum_{a=1}^{\lfloor s/2 \rfloor} \frac{1}{a} \right) \frac{1}{\Delta(\boldsymbol{\tau}) - \sqrt{\log N}/N} \le \frac{\log s}{\Delta(\boldsymbol{\tau}) - \sqrt{\log N}/N}.$$

In summary,

$$|\theta_m| \le \sqrt{\frac{N}{p}} \|\boldsymbol{\beta}\|_\infty + \frac{\|\boldsymbol{\beta}\|_\infty}{\sqrt{Np}} \frac{\log s}{\Delta(\boldsymbol{\tau}) - \sqrt{\log N}/N}$$

$$= \sqrt{r \log p} \left(1 + \frac{\log s}{N\Delta(\boldsymbol{\tau}) - \sqrt{\log N}} \right)$$

$$\le \sqrt{r \log p} \left(1 + \frac{\log s}{\log^2 N - \sqrt{\log N}} \right).$$

Similarly, when $p > C(\gamma, \alpha, r, \varepsilon)$, we have

(5.7) $$|\theta_m| \le \sqrt{r \log p}\,(1 + \varepsilon^2) \qquad \forall m \in D.$$

Step 3. In this step, we aim to give a uniform upper bound of θ_m for all $m \in D^c$. Straightforward calculation yields

$$|\theta_m| = \left| \sum_{1 \le l \le s} \frac{\tilde{\beta}_l}{\sqrt{Np}} \sum_{j=1}^N e^{2\pi i (j-1)((m-1)/q - (\tau_l - 1)/p)} \right|$$

$$\le \frac{\|\boldsymbol{\beta}\|_\infty}{\sqrt{Np}} \sum_{1 \le l \le s} \frac{|1 - e^{i 2\pi N((m-1)/q - (\tau_l - 1)/p)}|}{|1 - e^{i 2\pi ((m-1)/q - (\tau_l - 1)/p)}|}$$

$$\le \frac{\|\boldsymbol{\beta}\|_\infty}{\sqrt{Np}} \sum_{1 \le l \le s} \frac{1}{2d((m-1)/q, (\tau_l - 1)/p)}.$$

We now aim to bound $\sum_{1 \le l \le s} \frac{1}{2d((m-1)/q, (\tau_l - 1)/p)}$. We consider the position of $\frac{m-1}{q}$ on $T = [0, 1]/\{0 \sim 1\}$ relative to $\frac{\tau_1 - 1}{p}, \ldots, \frac{\tau_s - 1}{p}$. Suppose on $T = [0, 1]/\{0 \sim 1\}$, $\frac{m-1}{q}$ is located between $\frac{\tau_j - 1}{p}$ and $\frac{\tau_{j+1} - 1}{p}$ (recall that $\tau_{s+1} = \tau_1$). Since $m \in D^c$, we have $d(\frac{m-1}{q}, \frac{\tau_j - 1}{p}) \ge \frac{\sqrt{\log N}}{N}$ and $d(\frac{m-1}{q}, \frac{\tau_{j+1} - 1}{p}) \ge \frac{\sqrt{\log N}}{N}$. The next adjacent location parameters τ_{j-1} and τ_{j+2} satisfy $d(\frac{m-1}{q}, \frac{\tau_{j-1} - 1}{p}) \ge \Delta(\boldsymbol{\tau}) + \frac{\sqrt{\log N}}{N}$ and $d(\frac{m-1}{q}, \frac{\tau_{j+2} - 1}{p}) \ge \Delta(\boldsymbol{\tau}) + \frac{\sqrt{\log N}}{N}$, etc. Then we have

$$\sum_{1 \le l \le s} \frac{1}{2d((m-1)/q, (\tau_l - 1)/p)} \le \sum_{a=0}^{\lfloor (s-1)/2 \rfloor} \frac{1}{a\Delta(\boldsymbol{\tau}) + \sqrt{\log N}/N}$$

$$\le \frac{N}{\sqrt{\log N}} + \frac{\log s}{\Delta(\boldsymbol{\tau})}.$$

In summary,

$$|\theta_m| \le \frac{\|\boldsymbol{\beta}\|_\infty}{\sqrt{Np}} \left(\frac{N}{\sqrt{\log N}} + \frac{\log s}{\Delta(\boldsymbol{\tau})} \right) = \sqrt{r \log p} \left(\frac{1}{\sqrt{\log N}} + \frac{\log s}{\log^2 N} \right).$$

Similarly, when $p > C(\gamma, \alpha, r, \varepsilon)$, we have

$$(5.8) \qquad\qquad |\theta_m| \le \varepsilon^2 \sqrt{r \log p} \qquad \forall m \in D^c.$$

Step 4. We are now ready to derive a lower bound of $\mathbb{E}\mathrm{HC}(t)$. Recall that

$$(5.9) \qquad\qquad \mathrm{HC}(t) = \frac{\sum_{m=1}^q 1_{\{|v_m| > t\}} - q \bar{\Psi}(t)}{\sqrt{q \bar{\Psi}(t)(1 - \bar{\Psi}(t))}}.$$

By Lemma 5.2, we have

$$\mathbb{E}\mathrm{HC}(t) \ge \frac{\sum_{l=1}^s \mathbb{P}(|\theta_{m_l} + w_{m_l}| > t) - s \bar{\Psi}(t)}{\sqrt{q \bar{\Psi}(t)(1 - \bar{\Psi}(t))}}$$

$$\ge \frac{\sum_{l=1}^s C_0/(1+t) e^{-(t - |\theta_{m_l}|)_+^2} - s e^{-t^2}}{\sqrt{q \bar{\Psi}(t)(1 - \bar{\Psi}(t))}}.$$

By (5.6), we have

$$\min_{1 \le l \le s} |\theta_{m_l}| \ge (1 - \varepsilon^2) \sqrt{r \log p},$$

which implies

$$\mathbb{E}\mathrm{HC}(t) \ge \frac{s(C_0/(1+t) e^{-(t - (1-\varepsilon^2)\sqrt{r \log p})_+^2} - e^{-t^2})}{\sqrt{q \bar{\Psi}(t)(1 - \bar{\Psi}(t))}}.$$

Letting $t = \sqrt{\mu \log p}$, by $s = p^{1-\alpha}$, $N = p^{1-\gamma}$ and $q = N \lfloor \log N + 1 \rfloor$, there holds

$$(5.10) \quad \mathbb{E}\mathrm{HC}(\sqrt{\mu \log p}) \ge \frac{1}{\mathrm{polylog}(p)} p^{1/2 - \alpha + \gamma/2 + \mu/2 - (\sqrt{\mu} - (1-\varepsilon^2)\sqrt{r})_+^2},$$

where $\mathrm{polylog}(p)$ is a polynomial of $\log p$.

5.2.2. *Upper bound of* $\mathrm{Var}(\mathrm{HC}(t))$ *under the alternative.* By (5.7) and (5.8), we have

$$\begin{cases} \max_{1 \le m \le q} |\theta_m| \le (1 + \varepsilon^2) \sqrt{r \log p}, \\ \max_{m \in D^c} |\theta_m| \le \varepsilon^2 \sqrt{r \log p}. \end{cases}$$

By the definition of HC(t) as in (5.9), simple calculation yields

$$\text{Var HC}(t) = \frac{1}{q\bar{\Psi}(t)(1-\bar{\Psi}(t))} \sum_{1 \le a,b \le q} \text{cov}(1_{\{|\theta_a+w_a|>t\}}, 1_{\{|\theta_b+w_b|>t\}}).$$

By equation (5.3), when $d(\frac{a-1}{q}, \frac{b-1}{q}) \ge \frac{1}{N}$, we have

$$\left|\mathbb{E}(w_a\bar{w}_b)\right| \le \frac{1}{2Nd((a-1)/q,(b-1)/q)} \le \frac{1}{2}.$$

Then Lemma 5.3 implies

$$\text{cov}(1_{\{|\theta_a+w_a|>t\}}, 1_{\{|\theta_b+w_b|>t\}}) \le \frac{C_0 \exp(-((t-|\theta_a|)_+^2 + (t-|\theta_b|)_+^2)/2)(1+t)^2}{2Nd((a-1)/q,(b-1)/q)}.$$

On the other hand, when $d(\frac{a-1}{q}, \frac{b-1}{q}) < \frac{1}{N}$, Lemma 5.3 implies

$$\text{cov}(1_{\{|\theta_a+w_a|>t\}}, 1_{\{|\theta_b+w_b|>t\}}) \le e^{-(t-|\theta_a|)_+^2}.$$

Now we bound $\text{Var HC}(t)$ by controlling

$$S_1(t) = \frac{1}{q\bar{\Psi}(t)(1-\bar{\Psi}(t))}$$
$$\times \sum_{a \in D} \sum_{d((a-1)/q,(b-1)/q)<1/N} \text{cov}(1_{\{|\theta_a+w_a|>t\}}, 1_{\{|\theta_b+w_b|>t\}}),$$

$$S_2(t) = \frac{1}{q\bar{\Psi}(t)(1-\bar{\Psi}(t))}$$
$$\times \sum_{a \in D} \sum_{d((a-1)/q,(b-1)/q)\ge 1/N} \text{cov}(1_{\{|\theta_a+w_a|>t\}}, 1_{\{|\theta_b+w_b|>t\}}),$$

$$S_3(t) = \frac{1}{q\bar{\Psi}(t)(1-\bar{\Psi}(t))}$$
$$\times \sum_{\substack{a \in D^c \\ b \in D^c}} \sum_{d((a-1)/q,(b-1)/q)<1/N} \text{cov}(1_{\{|\theta_a+w_a|>t\}}, 1_{\{|\theta_b+w_b|>t\}}),$$

and

$$S_4(t) = \frac{1}{q\bar{\Psi}(t)(1-\bar{\Psi}(t))}$$
$$\times \sum_{\substack{a \in D^c \\ b \in D^c}} \sum_{d((a-1)/q,(b-1)/q)\ge 1/N} \text{cov}(1_{\{|\theta_a+w_a|>t\}}, 1_{\{|\theta_b+w_b|>t\}}).$$

By the symmetry between a and b, we have

$$\text{Var HC}(t) \le 2\big(S_1(t) + S_2(t)\big) + S_3(t) + S_4(t).$$

Step 1: *Upper bound for* $S_1(t)$. For fixed $a \in D$,

$$
\sum_{d((a-1)/q,(b-1)/q)<1/N} \mathrm{cov}(1_{\{|\theta_a+w_a|>t\}}, 1_{\{|\theta_b+w_b|>t\}}) \le \frac{2q}{N} e^{-(t-|\theta_a|)_+^2}
$$

$$
\le \frac{2q}{N} e^{-(t-\sqrt{r\log p}(1+\varepsilon^2))_+^2}.
$$

Notice that $|D| \le \frac{2qs\sqrt{\log N}}{N}$, we get

$$
S_1(t) \le \frac{2qs\sqrt{\log N}/N}{q\bar{\Psi}(t)(1-\bar{\Psi}(t))} \frac{2q}{N} e^{-(t-\sqrt{r\log p}(1+\varepsilon^2))_+^2}
$$

which implies

$$
S_1(\sqrt{\mu\log p}) \le \mathrm{polylog}(p) p^{-\alpha+\gamma+\mu-(\sqrt{\mu}-(1+\varepsilon^2)\sqrt{r})_+^2}.
$$

Step 2: *Upper bound for* $S_2(t)$. For fixed $a \in D$,

$$
\sum_{d((a-1)/q,(b-1)/q)\ge 1/N} \mathrm{cov}(1_{\{|\theta_a+w_a|>t\}}, 1_{\{|\theta_b+w_b|>t\}})
$$

$$
\le \sum_{d((a-1)/q,(b-1)/q)\ge 1/N} \frac{C_0 \exp(-((t-|\theta_a|)_+^2 + (t-|\theta_b|)_+^2)/2)(1+t)^2}{2Nd((a-1)/q,(b-1)/q)}
$$

$$
\le \frac{C_0(1+t)^2 e^{-(t-\sqrt{r\log p}(1+\varepsilon^2))_+^2}}{2N}
$$

$$
\times \sum_{d((a-1)/q,(b-1)/q)\ge 1/N} \frac{1}{d((a-1)/q,(b-1)/q)}
$$

$$
\le \frac{C_0(1+t)^2 e^{-(t-\sqrt{r\log p}(1+\varepsilon^2))_+^2}}{2N} 2\sum_{l=1}^{q} \frac{q}{l}
$$

$$
\le \frac{C_0 q \log q (1+t)^2 e^{-(t-\sqrt{r\log p}(1+\varepsilon^2))_+^2}}{N}.
$$

Notice that $|D| \le \frac{2qs\sqrt{\log N}}{N}$, we get

$$
S_2(t) \le \frac{2qs\sqrt{\log N}/N}{q\bar{\Psi}(t)(1-\bar{\Psi}(t))} \frac{C_0 q \log q (1+t)^2 e^{-(t-\sqrt{r\log p}(1+\varepsilon^2))_+^2}}{N},
$$

which implies

$$
S_2(\sqrt{\mu\log p}) \le \mathrm{polylog}(p) p^{-\alpha+\gamma+\mu-(\sqrt{\mu}-(1+\varepsilon^2)\sqrt{r})_+^2}.
$$

Step 3: *Upper bound for* $S_3(t)$. For fixed $a \in D^c$ and any $b \in \{1, \ldots, q\}$

$$\text{cov}(1_{\{|\theta_a + w_a| > t\}}, 1_{\{|\theta_b + w_b| > t\}}) \le e^{-(t - |\theta_a|)_+^2} \le e^{-(t - \varepsilon^2 \sqrt{r \log p})_+^2}.$$

Then

$$S_3(t) \le \frac{1}{q \bar{\Psi}(t)(1 - \bar{\Psi}(t))} \sum_{a \in D^c} \sum_{\substack{d((a-1)/q,(b-1)/q) < 1/N \\ b \in D^c}} e^{-(t - \varepsilon^2 \sqrt{r \log p})_+^2}$$

$$= \frac{q(2q/N)e^{-(t - \varepsilon^2 \sqrt{r \log p})_+^2}}{q \bar{\Psi}(t)(1 - \bar{\Psi}(t))},$$

which implies

$$S_3(\sqrt{\mu \log p}) \le \text{polylog}(p) \, p^{\mu - (\sqrt{\mu} - \varepsilon^2 \sqrt{r})_+^2}.$$

Step 4: *Upper bound for* $S_4(t)$. For fixed $a \in D^c$,

$$\sum_{\substack{b \in D^c \\ d((a-1)/q,(b-1)/q) \ge 1/N}} \text{cov}(1_{\{|\theta_a + w_a| > t\}}, 1_{\{|\theta_b + w_b| > t\}})$$

$$\le \sum_{\substack{b \in D^c \\ d((a-1)/q,(b-1)/q) \ge 1/N}} \frac{C_0 \exp(-((t - |\theta_a|)_+^2 + (t - |\theta_b|)_+^2)/2)(1 + t)^2}{2Nd((a-1)/q,(b-1)/q)}$$

$$\le \frac{C_0(1 + t)^2 e^{-(t - \varepsilon^2 \sqrt{r \log p})_+^2}}{2N}$$

$$\times \sum_{\substack{b \in D^c \\ d((a-1)/q,(b-1)/q) \ge 1/N}} \frac{1}{d((a-1)/q,(b-1)/q)}$$

$$\le \frac{C_0(1 + t)^2 e^{-(t - \varepsilon^2 \sqrt{r \log p})_+^2}}{2N} 2 \sum_{l=1}^{q} \frac{q}{l}$$

$$\le \frac{C_0 q \log q (1 + t)^2 e^{-(t - \varepsilon^2 \sqrt{r \log p})_+^2}}{N}.$$

Therefore, $S_4(t) \le \frac{q}{q \bar{\Psi}(t)(1 - \bar{\Psi}(t))} \frac{C_0 q \log q (1 + t)^2 e^{-(t - \varepsilon^2 \sqrt{r \log p})_+^2}}{N}$, which implies

$$S_4(\sqrt{\mu \log p}) \le \text{polylog}(p) \, p^{\mu - (\sqrt{\mu} - \varepsilon^2 \sqrt{r})_+^2}.$$

Step 5: *Summary*. In summary, there holds

$$\text{Var} \, \text{HC}(\sqrt{\mu \log p})$$

$$(5.11) \quad \le 2(S_1(\sqrt{\mu \log p}) + S_2(\sqrt{\mu \log p})) + S_3(\sqrt{\mu \log p}) + S_4(\sqrt{\mu \log p})$$

$$\le \text{polylog}(p) \left(p^{-\alpha + \gamma + \mu - (\sqrt{\mu} - (1 + \varepsilon^2)\sqrt{r})_+^2} + p^{\mu - (\sqrt{\mu} - \varepsilon^2 \sqrt{r})_+^2} \right).$$

5.2.3. *Detectable region under the alternative and the values of ε and μ.* By Chebyshev's inequality, we have

$$\mathbb{P}\big(\mathrm{HC}(\sqrt{\mu \log p}) < \mathbb{E}\mathrm{HC}(\sqrt{\mu \log p}) - (\log N)\big(\mathrm{Var}(\mathrm{HC}(\sqrt{\mu \log p}))\big)^{1/2}\big)$$
$$\leq \frac{1}{\log^2 N}.$$

By (5.10) and (5.11), to guarantee $\mathbb{P}(\mathrm{HC}(\sqrt{\mu \log p}) \leq \log^2 N) \leq \frac{1}{\log^2 N}$, it suffices to require that $p > C(\gamma, \alpha, r, \varepsilon, \mu)$ is sufficiently large, and

$$\begin{cases} \dfrac{1}{2} - \alpha + \dfrac{\gamma}{2} + \dfrac{\mu}{2} - (\sqrt{\mu} - (1-\varepsilon^2)\sqrt{r})_+^2 \\ \qquad > \dfrac{1}{2}(-\alpha + \gamma + \mu - (\sqrt{\mu} - (1+\varepsilon^2)\sqrt{r})_+^2), \\ \dfrac{1}{2} - \alpha + \dfrac{\gamma}{2} + \dfrac{\mu}{2} - (\sqrt{\mu} - (1-\varepsilon^2)\sqrt{r})_+^2 > \dfrac{1}{2}(\mu - (\sqrt{\mu} - \varepsilon^2\sqrt{r})_+^2) > 0, \end{cases}$$

which amounts to

(5.12) $$\begin{cases} 1 - \alpha > 2(\sqrt{\mu} - (1-\varepsilon^2)\sqrt{r})_+^2 - (\sqrt{\mu} - (1+\varepsilon^2)\sqrt{r})_+^2, \\ 1 - 2\alpha + \gamma > 2(\sqrt{\mu} - (1-\varepsilon^2)\sqrt{r})_+^2 - (\sqrt{\mu} - \varepsilon^2\sqrt{r})_+^2. \end{cases}$$

In order to find appropriate $\mu \in (0, 1-\gamma)$ and $\varepsilon > 0$ depending only on γ, α, r such that these two inequalities hold simultaneously, we will discuss three cases separately.

Case 1: $\frac{1+\gamma}{2} \leq \alpha < \frac{3+\gamma}{4}$ and $\alpha - \frac{1+\gamma}{2} < r \leq \frac{1-\gamma}{4}$. In this case, let $\mu = 4r(1-\varepsilon^2)^2$. Then both inequalities in (5.12) hold when we let $\varepsilon = 0$. By the continuity of the functions with respect to ε and the properties of open sets, we can choose a sufficiently small positive constant $C_0(\gamma, \alpha, r)$, such that when $\varepsilon = C_0(\gamma, \alpha, r) > 0$, both inequalities in (5.12) hold strictly.

Case 2: $\frac{1+\gamma}{2} \leq \alpha < \frac{3+\gamma}{4}$ and $r > \frac{1-\gamma}{4}$. In this case, let $\mu = (1-\gamma)(1-\varepsilon^2)^2$. Then both inequalities in (5.12) hold when we let $\varepsilon = 0$. Similarly, they also hold when $\varepsilon = C_0(\gamma, \alpha, r) > 0$.

Case 3: $\frac{3+\gamma}{4} \leq \alpha < 1$ and $r > (\sqrt{1-\gamma} - \sqrt{1-\alpha})^2$. In this case, let $\mu = (1-\gamma)(1-\varepsilon^2)^2$. Then both inequalities in (5.12) hold when we let $\varepsilon = 0$. Similarly, they also hold when $\varepsilon = C_0(\gamma, \alpha, r) > 0$.

In summary, for fixed $\frac{1+\gamma}{2} \leq \alpha < 1$ and $r > \rho_\gamma^*(\alpha)$, we can choose $\varepsilon > 0$ and $\mu \in (0, (1-\gamma)(1-\varepsilon)^2]$ only depending on γ, α, r such that such that both inequalities in (5.12) hold. Notice that $t = \sqrt{\mu \log p}$ lies in the domain of $\mathrm{HC}(t)$, that is, $[1, \sqrt{\log \frac{N}{3}}]$. Then when $p > C(\alpha, \gamma, r)$, we have the inequality $\mathbb{P}(\mathrm{HC}(\sqrt{\mu \log p}) \leq \log^2 N) \leq \frac{1}{\log^2 N}$, and hence $\mathbb{P}(\mathrm{HC}^* \leq \log^2 N) \leq \frac{1}{\log^2 N}$. Since

$C(\alpha, \gamma, r)$ is independent of the choice of $(\boldsymbol{\tau}, \tilde{\boldsymbol{\beta}})$, we have

$$\lim_{p \to \infty} \max_{(\boldsymbol{\tau}, \tilde{\boldsymbol{\beta}}) \in \Gamma(p, N, s, r)} \mathbb{P}_{(\boldsymbol{\tau}, \tilde{\boldsymbol{\beta}})}(H_0 \text{ is failed to reject}) = 0.$$

5.2.4. *Upper bound of* HC* *under the null.* Under the null, for $m = 1, \ldots, q$ we have $v_m = w_m$. By (5.4), for any $u = 1, \ldots, L$, the variables $v_u, v_{u+L},$ $v_{u+2L}, \ldots, v_{u+(N-1)L}$ are i.i.d. standard complex normal variables. This implies that $1_{\{|v_u| \geq t\}}, 1_{\{|v_{u+L}| \geq t\}}, \ldots, 1_{\{|v_{u+(N-1)L}| \geq t\}}$ are i.i.d. Bernoulli random variables with parameter $\bar{\Psi}(t) = e^{-t^2}$.

By Lemma 5.4, for any u, we have

$$\mathbb{P}\left(\sup_{1 \leq t \leq \sqrt{\log N/3}} \frac{\sum_{j=1}^{N} 1_{\{|v_{u+(j-1)L}| > t\}} - N\bar{\Psi}(t)}{\log N \sqrt{N\bar{\Psi}(t)(1 - \bar{\Psi}(t))}} > C_1 \right) < \frac{1}{\log^2 N},$$

provided $N > N_0$. Therefore,

$$\mathrm{HC}^* = \sup_{1 \leq t \leq \sqrt{\log N/3}} \frac{1}{\sqrt{L}} \sum_{u=1}^{L} \frac{\sum_{j=1}^{N} 1_{\{|v_{u+(j-1)L}| > t\}} - N\bar{\Psi}(t)}{\sqrt{N\bar{\Psi}(t)(1 - \bar{\Psi}(t))}}$$

$$\leq \frac{1}{\sqrt{L}} \sum_{u=1}^{L} \sup_{1 \leq t \leq \sqrt{\log N/3}} \frac{\sum_{j=1}^{N} 1_{\{|v_{u+(j-1)L}| > t\}} - N\bar{\Psi}(t)}{\sqrt{N\bar{\Psi}(t)(1 - \bar{\Psi}(t))}} \leq \sqrt{L} C_1 \log N$$

with probability at least $1 - \frac{L}{\log^2 N}$. Since $L = \lfloor \log N + 1 \rfloor$ and $N = p^{1-\gamma}$, we have

$$\lim_{p \to \infty} \mathbb{P}(H_0 \text{ is rejected}) = \lim_{p \to \infty} \mathbb{P}(\mathrm{HC}^* > \log^2 N) = 0.$$

SUPPLEMENTARY MATERIAL

Supplement to "Global testing against sparse alternatives in time-frequency analysis" (DOI: 10.1214/15-AOS1412SUPP; .pdf). We give in [11] the proofs to Lemmas 5.2, 5.3 and Theorem 2.2.

REFERENCES

[1] AHDESMAKI, M., LAHDESMAKI, H., PEARSON, R., HUTTUNEN, H. and YLI-HARJA, O. (2005). Robust detection of periodic time series measured from biological systems. *BMC Bioinformatics* **6** 117.

[2] AHDESMAKI, M., LAHDESMAKI, H. and YLI-HARJA, O. (2007). Robust Fisher's test for periodicity detection in noisy biological time series. In *GENSIPS, IEEE International Workshop on* 1–4. Tuusula, Finland.

[3] ALEXANDER, K. S. (1987). Rates of growth and sample moduli for weighted empirical processes indexed by sets. *Probab. Theory Related Fields* **75** 379–423. MR0890285

[4] ARIAS-CASTRO, E., CANDÈS, E. J., HELGASON, H. and ZEITOUNI, O. (2008). Searching for a trail of evidence in a maze. *Ann. Statist.* **36** 1726–1757. MR2435454

[5] ARIAS-CASTRO, E., CANDÈS, E. J. and PLAN, Y. (2011). Global testing under sparse alternatives: ANOVA, multiple comparisons and the higher criticism. *Ann. Statist.* **39** 2533–2556. MR2906877

[6] ARIAS-CASTRO, E., DONOHO, D. L. and HUO, X. (2005). Near-optimal detection of geometric objects by fast multiscale methods. *IEEE Trans. Inform. Theory* **51** 2402–2425. MR2246369

[7] BHASKAR, B. N., TANG, G. and RECHT, B. (2013). Atomic norm denoising with applications to line spectral estimation. *IEEE Trans. Signal Process.* **61** 5987–5999. MR3138795

[8] BØLVIKEN, E. (1983). New tests of significance in periodogram analysis. *Scand. J. Stat.* **10** 1–9. MR0711329

[9] BROCKWELL, P. J. and DAVIS, R. A. (2009). *Times Series: Theory and Methods*, 2nd ed. Springer, Berlin.

[10] CADZOW, J. (1988). Signal enhancement—a composite property mapping algorithm. *IEEE Trans. Acoust. Speech Signal Process.* **36** 49–62.

[11] CAI, T., ELDAR, Y. C. and LI, X. (2016). Supplement to "Global testing against sparse alternatives in time-frequency analysis." DOI:10.1214/15-AOS1412SUPP.

[12] CAI, T. T., JENG, X. J. and JIN, J. (2011). Optimal detection of heterogeneous and heteroscedastic mixtures. *J. R. Stat. Soc. Ser. B Stat. Methodol.* **73** 629–662. MR2867452

[13] CAI, T. T., JIN, J. and LOW, M. G. (2007). Estimation and confidence sets for sparse normal mixtures. *Ann. Statist.* **35** 2421–2449. MR2382653

[14] CAI, T. T. and WU, Y. (2014). Optimal detection of sparse mixtures against a given null distribution. *IEEE Trans. Inform. Theory* **60** 2217–2232. MR3181520

[15] CANDÈS, E. J. and FERNANDEZ-GRANDA, C. (2013). Super-resolution from noisy data. *J. Fourier Anal. Appl.* **19** 1229–1254. MR3132912

[16] CANDÈS, E. J. and FERNANDEZ-GRANDA, C. (2014). Towards a mathematical theory of super-resolution. *Comm. Pure Appl. Math.* **67** 906–956. MR3193963

[17] CHEN, J. (2005). Identification of significant genes in microarray gene expression data. *BMC Bioinformatics* **6** 286.

[18] CHEN, S. S. and DONOHO, D. L. (1998). Application of basis pursuit in spectrum estimation. In *Conference on Acoustics, Speech and Signal Processing, Vol.* 3. Seattle, WA.

[19] CHIU, S.-T. (1989). Detecting periodic components in a white Gaussian time series. *J. Roy. Statist. Soc. Ser. B* **51** 249–259. MR1007457

[20] DAVIES, R. B. (1987). Hypothesis testing when a nuisance parameter is present only under the alternative. *Biometrika* **74** 33–43. MR0885917

[21] DICKER, L. H. (2014). Variance estimation in high-dimensional linear models. *Biometrika* **101** 269–284. MR3215347

[22] DJURIĆ, P. M. (1996). A model selection rule for sinusoids in white Gaussian noise. *IEEE Trans. Signal Process.* **44** 1744–1751.

[23] DONOHO, D. and JIN, J. (2004). Higher criticism for detecting sparse heterogeneous mixtures. *Ann. Statist.* **32** 962–994. MR2065195

[24] DONOHO, D. L. (1992). Superresolution via sparsity constraints. *SIAM J. Math. Anal.* **23** 1309–1331. MR1177792

[25] DUARTE, M. F. and BARANIUK, R. G. (2013). Spectral compressive sensing. *Appl. Comput. Harmon. Anal.* **35** 111–129. MR3053749

[26] FANNJIANG, A. and LIAO, W. (2012). Coherence pattern-guided compressive sensing with unresolved grids. *SIAM J. Imaging Sci.* **5** 179–202. MR2902661

[27] FISHER, R. A. (1929). Tests of significance in harmonic analysis. *Proceedings of Royal Society, Ser. A* **125** 54–59.

[28] FULLER, W. A. (1976). *Introduction to Statistical Time Series*. Wiley, New York. MR0448509

[29] GINÉ, E. and KOLTCHINSKII, V. (2006). Concentration inequalities and asymptotic results for ratio type empirical processes. *Ann. Probab.* **34** 1143–1216. MR2243881

[30] GLYNN, E. F., CHEN, J. and MUSHEGIAN, A. R. (2006). Detecting periodic patterns in unevenly spaced gene expression time series using Lomb–Scargle periodograms. *Bioinformatics* **22** 310–316.

[31] HALL, P. and JIN, J. (2010). Innovated higher criticism for detecting sparse signals in correlated noise. *Ann. Statist.* **38** 1686–1732. MR2662357

[32] HU, L., SHI, Z., ZHOU, J. and FU, Q. (2012). Compressed sensing of complex sinusoids: An approach based on dictionary refinement. *IEEE Trans. Signal Process.* **60** 3809–3822. MR2951227

[33] HUA, Y. and SARKAR, T. K. (1990). Matrix pencil method for estimating parameters of exponentially damped/undamped sinusoids in noise. *IEEE Trans. Acoust. Speech Signal Process.* **38** 814–824. MR1051029

[34] INGSTER, YU. I. (1998). Minimax detection of a signal for l^n-balls. *Math. Methods Statist.* **7** 401–428 (1999). MR1680087

[35] INGSTER, Y. I., TSYBAKOV, A. B. and VERZELEN, N. (2010). Detection boundary in sparse regression. *Electron. J. Stat.* **4** 1476–1526. MR2747131

[36] JUDITSKY, A. and NEMIROVSKI, A. (2015). On detecting harmonic oscillations. *Bernoulli* **21** 1134–1165. MR3338659

[37] KAY, S. M. (1998). *Fundamentals of Statistical Signal Processing*: *Detection Theory*. Prentice Hall, Upper Saddle River, NJ.

[38] KNIGHT, W. C., PRIDHAM, R. G. and KAY, S. M. (1981). Digital signal processing for sonar. *Proc. IEEE* **69** 1451–1506.

[39] LEADBETTER, M. R., LINDGREN, G. and ROOTZÉN, H. (1983). *Extremes and Related Properties of Random Sequences and Processes*. Springer, New York. MR0691492

[40] LI, J. and SIEGMUND, D. (2015). Higher criticism: *p*-values and criticism. *Ann. Statist.* **43** 1323–1350. MR3346705

[41] LI, W. V. and SHAO, Q.-M. (2002). A normal comparison inequality and its applications. *Probab. Theory Related Fields* **122** 494–508. MR1902188

[42] NADLER, B. and KONTOROVICH, A. (2011). Model selection for sinusoids in noise: Statistical analysis and a new penalty term. *IEEE Trans. Signal Process.* **59** 1333–1345. MR2807736

[43] PRONY, R. (1795). Essai expérimental et analytique: Sur les lois de la dilatabilité de fluides élastique et sur celles de la force expansive de la vapeur de l'alkool, à différentes températures. *J. Éc. Polytech.* **1** 24–76.

[44] QUINN, B. G. and HANNAN, E. J. (2001). *The Estimation and Tracking of Frequency. Cambridge Series in Statistical and Probabilistic Mathematics* **9**. Cambridge Univ. Press, Cambridge. MR1813156

[45] QUINN, B. G. and KOOTSOOKOS, P. J. (1994). Threshold behavior of the maximum likelihood estimator of frequency. *IEEE Trans. Signal Process.* **42** 3291–3294.

[46] ROY, R. and KAILATH, T. (1990). ESPRIT—estimation of signal parameters via rotational invariance techniques. In *Signal Processing*, *Part II. IMA Vol. Math. Appl.* **23** 369–411. Springer, New York. MR1058066

[47] RUBIN-DELANCHY, P. and WALDEN, A. T. (2008). Kinematics of complex-valued time series. *IEEE Trans. Signal Process.* **56** 4189–4198. MR2517167

[48] SCHMIDT, R. (1986). Multiple emitter location and signal parameter estimation. *IEEE Trans. Antennas and Propagation* **34** 276–280.

[49] SIEGEL, A. F. (1980). Testing for periodicity in a time series. *J. Amer. Statist. Assoc.* **75** 345–348.

[50] SKOLNIK, M. I. (1980). *Introduction to Radar Systems*. McGraw-Hill, New York.

[51] SYKULSKI, A. M., OLHEDE, S. C., LILLY, J. M. and EARLY, J. J. (2013). The Whittle likelihood for complex-valued time series. Preprint.

[52] TANG, G., BHASKAR, B. N. and RECHT, B. (2015). Near minimax line spectral estimation. *IEEE Trans. Inform. Theory* **61** 499–512. MR3299978

[53] VAN ZUIJLEN, M. C. A. (1978). Properties of the empirical distribution function for independent nonidentically distributed random variables. *Ann. Probab.* **6** 250–266. MR0474624

[54] VAN TREES, H. L. (1992). *Detection, Estimation, and Modulation Theory, Part* 3: *Radar-Sonar Signal Processing and Gaussian Signals in Noise*. Wiley, New York.

[55] WHALEN, A. D. (1995). *Detection of Signals in Noise*. Academic Press, New York.

[56] WICHERT, S., FOKIANOS, K. and STRIMMER, K. (2004). Identifying periodically expressed transcripts in microarray time series data. *Bioinformatics* **20** 5–20.

T. T. CAI
DEPARTMENT OF STATISTICS
THE WHARTON SCHOOL
UNIVERSITY OF PENNSYLVANIA
400 JON M. HUNTSMAN HALL
3730 WALNUT STREET
PHILADELPHIA, PENNSYLVANIA 19104-6340
USA
E-MAIL: tcai@wharton.upenn.edu

Y. C. ELDAR
DEPARTMENT OF ELECTRICAL ENGINEERING
TECHNION—ISRAEL INSTITUTE
   OF TECHNOLOGY
HAIFA 32000
ISRAEL
E-MAIL: yonina@ee.technion.ac.il

X. LI
DEPARTMENT OF STATISTICS
UNIVERSITY OF CALIFORNIA, DAVIS
4109 MATHEMATICAL SCIENCES
DAVIS, CALIFORNIA 95616
USA
E-MAIL: xdgli@ucdavis.edu